Journal of the European Ceramic Society 22 (2002) 2197–2208

www.elsevier.com/locate/jeurceramsoc

Effect of particle size distribution on sintering of agglomerate-free submicron alumina powder compacts

J. Ma[a], L.C. Lim[b,*]

[a]*School of Materials Engineering, Nanyang Technological University, Nanyang Avenue, Singapore 639798, Singapore*
[b]*Department of Mechanical Engineering, National University of Singapore, 10, Kent Ridge Crescent, Singapore 119260, Singapore*

Received 21 March 2001; received in revised form 10 December 2001; accepted 28 December 2001

Abstract

Experiments were performed with colloidally processed submicron alumina powders to investigate the effect of particle size distribution on their sintering characteristics. The results showed that in the absence of agglomerates and macroscopic size segregation, a broader particle size distribution leads to two opposing phenomena during sintering—enhanced overall sintering characteristics and a higher degree of local differential densification. The former is a result of both the higher initial green density and smaller isolated pores in the final stage of sintering brought about by enhanced grain growth during the intermediate stage. The latter is promoted by a higher degree of variation in local particle packing and may negate the enhanced sintering effect at sufficiently broad particle size distribution. There therefore exists an optimum range of particle size distribution for best sinterability. Since the optimum particle size distribution may vary considerably even for a given powder system, depending on the compaction technique and conditions used, narrow size distribution powder is preferred to monosized or broad size distribution powders for high sinterability and microstructure control of powder compacts, provided that agglomerates in the starting powder are removed by appropriate means. For the agglomerate-free, submicron alumina powder system studied, the optimum particle size distribution was found to have a geometric standard deviation value lying in between 1.6 and 1.9.

Keywords: Al_2O_3; Grain growth; Particle size distribution; Porosity; Sintering

1. Introduction

Sintering of ceramic powder compacts has been extensively investigated due to its technological importance. Although it has been suggested that monosized powders are preferred in producing dense, uniform, fine-grained microstructure,[1–4] most powders for practical purposes possess certain size distributions, both to enhance sintering and to minimise overall shrinkage.

Experimental works on sintering of powders of continuous size distribution have been reported by earlier researchers but the results are not altogether consistent. Petterson and Benson[5] found that blends of copper spheres with broader particle size distributions sintered more rapidly. They also noted that narrow size distribution compacts contained fewer but larger pores while the broad size distribution compacts had more but smaller pores. In a subsequent work, Petterson and Griffin[6] reported that in tungsten, their narrowest and broadest size distribution powders showed enhanced sinterability than those of intermediate size distributions. They also noted that the narrowest size distribution powder yielded a much more uniform pore structures than those of broader size distributions.

Working with commercial alumina powders, Ting and Lin[7] noted that the compact prepared from powder of a broader size distribution exhibited a higher sintering rate prior to the occurrence of grain growth but a lower densification rate after grain growth took place. The grain size/density trajectories revealed that the broader size distribution powder resulted in inferior overall sinterability, which agrees with the prediction of their model.[8]

It should be mentioned that in the above works, commercial powders were used and the powders were consolidated by the dry-pressing technique. This could lead to complication in result interpretation because other green microstructural features, such as agglomerates, are known to exert a dominant influence on the

* Corresponding author. Fax: +65-779-1459.
E-mail address: mpelimlc@nus.edu.sg (L.C. Lim).

0955-2219/02/$ - see front matter
PII: S0955-2219(02)00009-2

densification behaviour of powder compacts,[9–13] thereby masking the effect caused by the size distribution.

To overcome the problem associated with agglomerates, a recent trend in ceramic processing has been the use of colloidal processing techniques.[14–18] Using such techniques, Roosen and Bowen[17] and Hay et al.[18] showed that colloidally classified, narrow size distribution powders gave consistently more uniform and finer pore structures and were sintered to full density at relatively low temperatures with a uniform and fine-grained microstructure. A similar finding was also reported by Shiau et al.[19] and Lim et al.[20]

In the above works, the as-received powders, which also had a broader particle size distribution, were used as the reference for comparison. Since the as-received, unclassified powders also contained agglomerates, we are again faced with the uncertainty of whether the reported observations reflect the true effect of particle size distribution or agglomerate related sintering phenomenon.

Using the colloidal route, Yeh and Sacks[21] prepared two agglomerate-free alumina compacts of the same mean particle size but different size distributions of 1.3 and 2.4 in geometric standard deviation (GSD), respectively. (GSD can be obtained by dividing the mean particle size by the particle size at 0.8 weight fraction.) They showed that the compact made from the broader particle size distribution powder gave a higher green density and improved densification behaviour during the initial stage of sintering. However, the densification rate of such a compact decreased faster on continued sintering; and, both compacts gave comparable end density and resultant grain size on further sintering. They therefore concluded that there is no advantage using powder of narrow size distributions for it has a lower starting green density, hence larger overall shrinkage.

In a recent work with near-monosized agglomerate-free submicron alumina compacts, Lim et al.[22] showed that despite being agglomerate-free to start with, agglomeration of particles still occurred during sintering due to the local differential densification effect produced by the different co-ordination numbers of individual particles. This led to the formation of channel-like pores, which then evolved into smaller isolated pores before they were eliminated on further sintering. Their results further showed that grain growth is necessary for further densification at the final stage of sintering.

In general, a broader particle size distribution is expected to lead to a higher green density due to the gap filling ability of the fine particles. This in turn increases the average coordination number of particles, leading to enhanced sintering. A broader particle size distribution also promotes grain growth,[25,26] which in turn would modify the evolution of pores, hence the densification behaviour of the compact.[23,24,27] On the other hand, too broad a particle size distribution may cause the sintering characteristics of the compact to deteriorate due to the low-sintering characteristic of the much coarser particles and increased structural inhomogeneity as a result of size segregation, either at macroscopic or microscopic level.[11,28–37]

A question thus arises as to what size distribution is optimum for best sinterability of powder compacts. The present work attempts to answer this question by performing a detailed study on the microstructural evolution of powder compacts of different particle size distributions. The compacts were processed colloidally to get rid of the agglomerates and the particle size distribution width was varied in small steps to enable subtle differences in the development of pore and grain structures in the compacts to be followed closely.

2. Experimental procedure

Powder compacts from powders of different particle size distributions were prepared by mixing three different 99.99% pure alumina powders (i.e. AKP20, AKP30 and AKP53 from Sumitomo Chemical Co., Japan) in appropriate proportions. The fractions of each powder type needed were estimated from the size distribution and contributing weight fraction of each powder type. The designed powders had a mean particle size of 0.4 μm but of different GSDs in size distribution. Altogether five different particle size distributions were studied, corresponding to expected GSDs of 1.2, 1.4, 1.6, 1.9 and 2.1, respectively.

All the powder mixtures were colloidally processed to get rid of the agglomerates; namely, aqueous suspensions containing 30 vol.% solid content were prepared and ultrasonicated at pH = 2.4, which gives the well-dispersed state, and then left in a quiescent environment for 24 h to allow the hard agglomerates to settle out via sedimentation (see Refs. 20 and 22 for details). The remaining suspension was then siphoned off and the powder mixture in it was compacted in a fixed-angle ultracentrifuge. To minimise potential size segregation, a large centrifugal force of 200,000 g was used, g being the acceleration due to gravitation, and the suspension height was keep no larger than 30 mm. A solid centrifuged cake with a clear supernatant was obtained in all cases. The cakes measured about 11 mm in average height, which, after drying, could be easily removed from the polycarbonate test tube by tapping. The dried compacts were pre-fired at 800 °C for about 40 min.

The particle size distributions in the compacts were examined by notching the pre-fired compacts with a low-speed diamond cutter and then breaking each into two halves with care. They were then gold coated and examined under the scanning electron microscope (SEM). The particle size distributions were quantified

from the SEM micrographs using the section-chord method. Similar results were obtained from both the fracture and as-cut surfaces of respective pre-fired compact, suggesting that the compacts were strong enough for handling after the pre-firing.

All the pre-fired compacts were cut into rectangular blocks of approximately 5×5×8 mm in dimensions, which removed at lease 1.5 mm thick of material each from the top and bottom layers of the centrifuged cake to further minimise potential size segregation effect. Green densities were taken by dividing the weight of the compact by its dimensions, measured to ±0.01 mg and ±0.01 mm accuracy, respectively.

The compacts were sintered at 1300, 1400 and 1500 °C for increasing length of time in a vacuum furnace. The specimens were heated from room temperature to the sintering temperature at a rate of 20 °C/min. Then, they were soaked at the temperature for the required time period, followed by furnace cooling to room temperature.

Careful examinations were carried out to follow the microstructural evolution during sintering of the compacts with GSD = 1.2 and 1.6. These two compacts were selected because the former represents near-monosized powder while the latter exhibits the best sintering characteristics (see Section 3.2). A lower sintering temperature of 1250 °C was used in this case to enable the microstructural development to be followed more closely. After sintering for pre-determined lengths of time, the specimens were first sectioned by means of a diamond-impregnated blade at a low cutting speed of 150 rpm to minimize pullouts and other cutting defects. Then, the surfaces of interest were polished with diamond paste to mirror-finish and the samples were thermally etched at 1150 °C for 4 h to reveal the grain structure. After which, they were gold coated and examined under the SEM.

3. Results

3.1. Characteristics of green compacts

Fig. 1 shows the measured particle size distributions of the five compacts investigated. All the powder compacts had a continuous size distribution with their GSDs conformed reasonably to the designed values.

The green densities of the compacts with different particle size distributions are shown in Fig. 2. It can be seen that over the range of particle size distribution studied, the green density of the compacts increases linearly with particle size distribution. This can be attributed to the smaller particles filling up the interstices between the larger ones, thereby increasing the overall density of the compact.

3.2. Sinterability study

The densification behaviours of all five powder compacts at different temperatures are shown in Fig. 3. Compared with the compact of near-monosized distribution (dashed curves), all compacts with broader size distributions showed enhanced densification behaviour at the initial stage of sintering. However, their densification rates decreased more rapidly as sintering proceeded into the intermediate stage.

The results also show that over the range of particle size distribution investigated, all broader size distribution compacts exhibited superior overall sintering characteristics than the near-monosized compact. This can

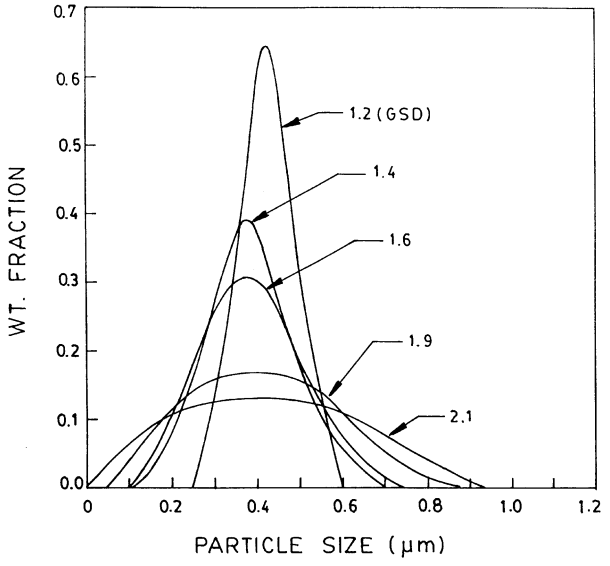

Fig. 1. Measured particle size distributions of powder compacts of different GSDs used in the present work.

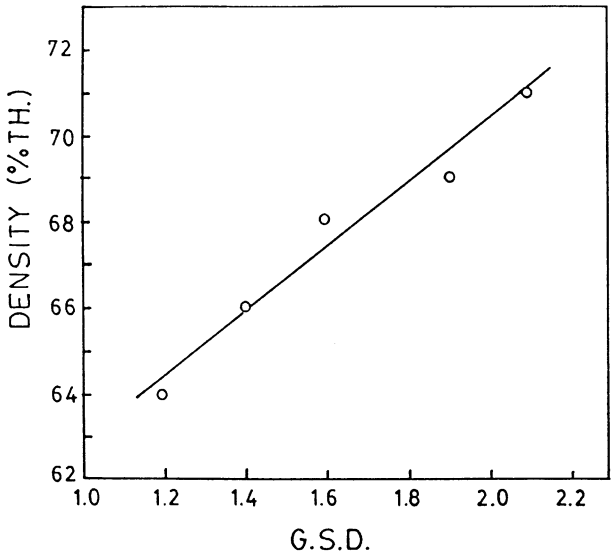

Fig. 2. Green density of compacts at different particle size distributions.

be more readily seem from Fig. 4, which gives the sintering temperatures required to produce compacts of 96 and 98% relative density in 1 h, respectively. The compacts with GSD = 1.6 and 1.9 possess the best sinterability among all the five types of powder compacts studied in the present work.

3.3. Grain growth characteristics

The grain growth curves for all the five compacts at 1300 °C are given in Fig. 5. Note the higher initial average grain sizes for compacts with smaller GSDs. This is because GSD is expressed in terms of weight frequency. Hence, for a given mean particle size, with increasing GSD, the number frequencies of the fine particles will increase accordingly relative to the coarse ones. This will lead to a smaller average grain size when measured from the SEM micrographs.

Fig. 5 shows that for compacts with GSD $\leqslant$1.4, grain growth was negligible during the initial first hour at 1300 °C. On the other hand, for compacts of broader size distribution (i.e. GSD $\geqslant$1.6), grain growth was appreciable during the first hour at temperature. However, the grain growth rate in the latter compacts diminished after 2 h at temperature.

The grain size-density trajectories of the various compacts are given in Fig. 6. This figure confirms the superior sinterability of the GSD = 1.6 and 1.9 compacts over that of the near-monosized (GSD = 1.2) and broader size distribution compact (GSD = 2.1). This figure further shows that although perceptible differences in grain growth behaviour were noted between the

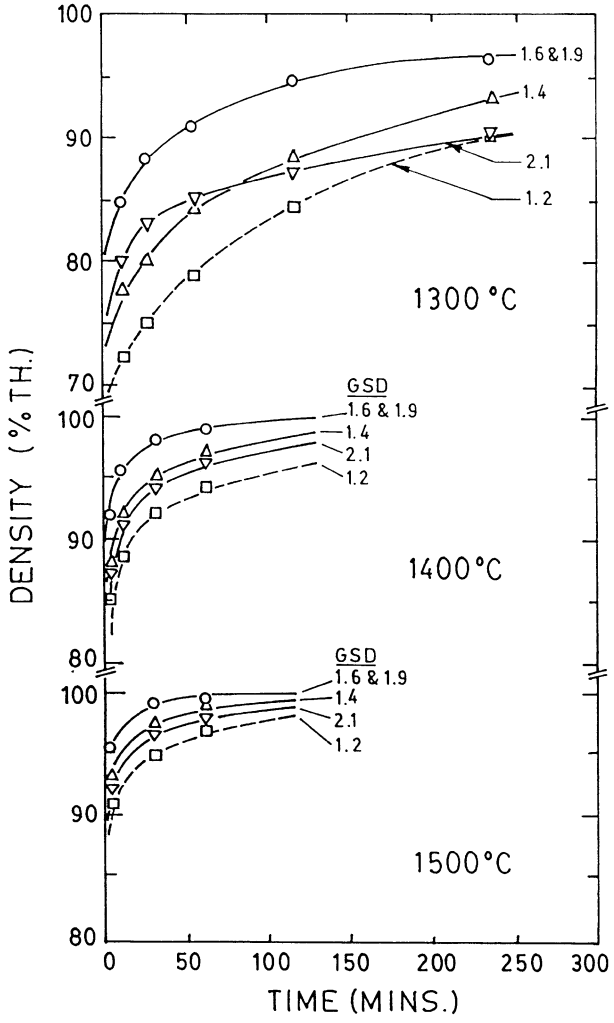

Fig. 3. Densification curves of compacts of different particle size distributions at different temperatures. The dashed curves pertain to that of near-monosized powder compacts.

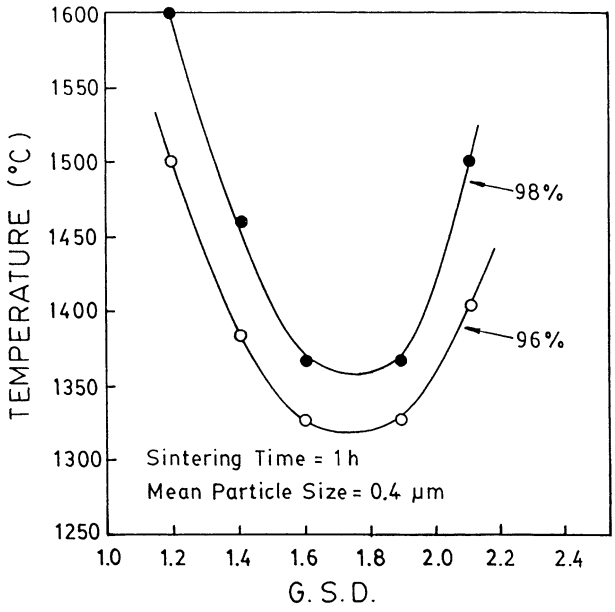

Fig. 4. Sinterability of alumina compacts of different particle size distributions as deduced from Fig. 3.

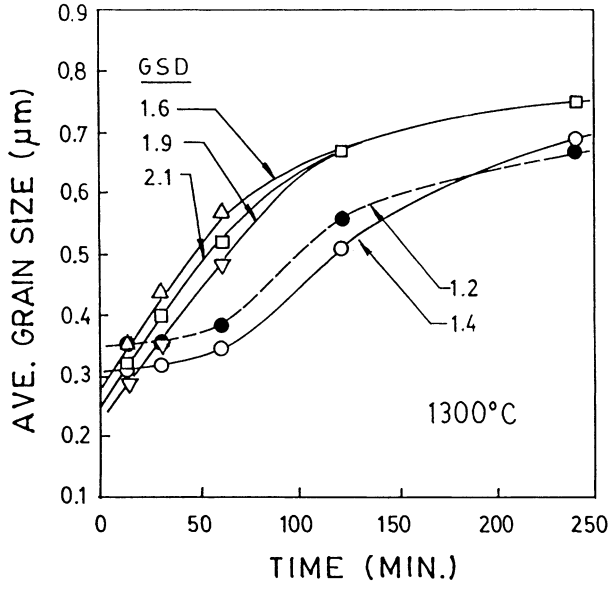

Fig. 5. Grain growth curves at 1300 °C for all compacts. The dashed curve pertains to that of near-monosized powder compact.

narrow (GSD = 1.2 and 1.4) and broad size distribution (GSD = 1.6, 1.9 and 2.1) compacts at the intermediate stage of sintering, the differences lessened as sintering progressed. After 1 h at 1500 °C, all compacts registered a comparable grain size of about 2.4 μm. This observation suggests that within the range of particle size distribution investigated, the resultant grain size at the final stage of sintering is very much determined by the sintering condition used but not the particle size distribution of the starting powder. Both the GSD = 1.6 and 1.9 compacts were fully dense (i.e. >99.5% in relative density) after 1 h at 1500 °C, which compares favourably with a relative density of 97% for the near-monosized (GSD = 1.2) compact, and of 99% and 98% for the GSD = 1.4 and 2.1 compacts, respectively (Fig. 6).

3.4. Microstructural study

Detailed microstructural studies revealed that all the powder compacts went through similar stages of microstructural development, as illustrated in Fig. 7 which were taken from the GSD = 1.6 compact sintered at 1250 °C. At this temperature, the evolution of the sintering microstructure took place at a slower pace, enabling us to follow their development more closely.

During the initial stage of sintering, local densification occurred among clusters of particles, causing the formation of sintering-induced agglomerates and the opening up of pores among them (Fig. 7a and b). The opened pores formed between the agglomerates generally had a channel-like shape. As sintering continued, the channel-like inter-agglomerate pores gradually developed into smaller isolated pores (Fig. 7c and d). These isolated pores were rather stable and were removed fairly slowly on further sintering (Fig. 7e and f). The sintering rate also slowed down substantially at this stage. The above observations are consistent with an earlier finding obtained with near-monosized, agglomerate-free alumina compacts with a mean particle size of 0.18 μm.[22]

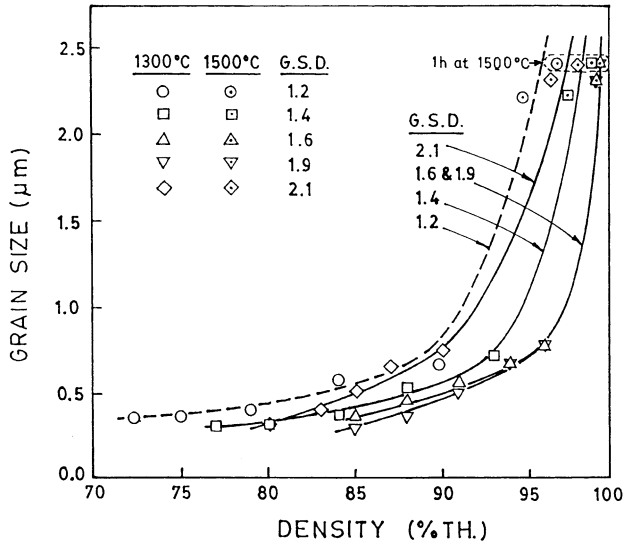

Fig. 6. Grain size-density trajectories of all compacts studied. The dashed curve pertains to that of near-monosized powder compact.

3.5. Evolution of pore structures

For the ease of result presentation and analysis, the pores observed were classified into the following four major types: open inter-particle (Type 1) pores which exist between the particles in the green state and persist during the early stage of sintering; closed inter-particle (Type 2) pores which are formed as a result of the closure of Type 1 pores; open inter-agglomerate (Type 3) pores which are the large channel-like pores formed as a result of the sintering-induced agglomeration of particles; and closed inter-agglomerate (Type 4) pores which result from the closure of Type 3 pores. Typical examples of the various types of pores are given in Fig. 7. The distributions of pore type and size, the latter expressed in equivalent diameter, in the various compacts were quantified from the SEM micrographs. At least 200 pores were counted in each compact. As Type 1 and 2 pores are difficult to distinguish from the micrographs, they are illustrated as combined Type 1/2 pores in the pore type and size measurement.

The evolution of different types of pores and their size distributions during the sintering process in the powder compacts with GSD = 1.2 and 1.6 are shown in Figs. 8 and 9, respectively. Despite the similarity in the evolution sequence of pore structure, two distinctive features can be noted between the two powder compacts. Firstly, the evolution process took place in a shorter time for the GSD = 1.6 compact as compared to the GSD = 1.2 compact. Secondly, the closed isolated Type 4 pores which formed at the final stage of sintering were finer for the GSD = 1.6 compact.

3.6. Pore structure at fixed relative density

More importantly, the present work showed that over the range of size distribution and temperature investigated, all the four broader size distribution compacts exhibited improved overall sinterability than the near-monosized compact; namely, they were sintered to >96% relative density at lower temperatures (Fig. 4). This is most pronounced for compacts having the optimum range of particle size distribution, i.e. with GSD = 1.6 and 1.9, which were sintered to full density at temperatures at least 200 °C lower than that required for the near-monosized compact. The above observation is consistent with that of Yeh and Sacks,[21] who worked with similar powders but of two different particle size distributions of GSD = 1.3 and 2.4.

To provide a better insight into the above-observed phenomenon, the pore size distribution of the five different GSD powder compacts sintered at 1300 °C to a fixed relative density of 85% were quantified. Note that at this stage, only Type 4 pores were present in all the compacts. The results are shown in Fig. 10.

It can be seen from this figure that at 85% relative density, the near-monosized compact (i.e. GSD = 1.2) shows a good distribution of Type 4 pores with some $\geqslant 0.1$ μm in equivalent diameter. With broader particle size distribution, the size of Type 4 pores decreases accordingly. And, the compacts with GSD = 1.6 and 1.9 were found to have the finest Type 4 pores. It is interesting to note that with a further broadening in particle size distribution (i.e. GSD = 2.1), the Type 4 pores again display a distribution comparable to that found in the near-monosized compact.

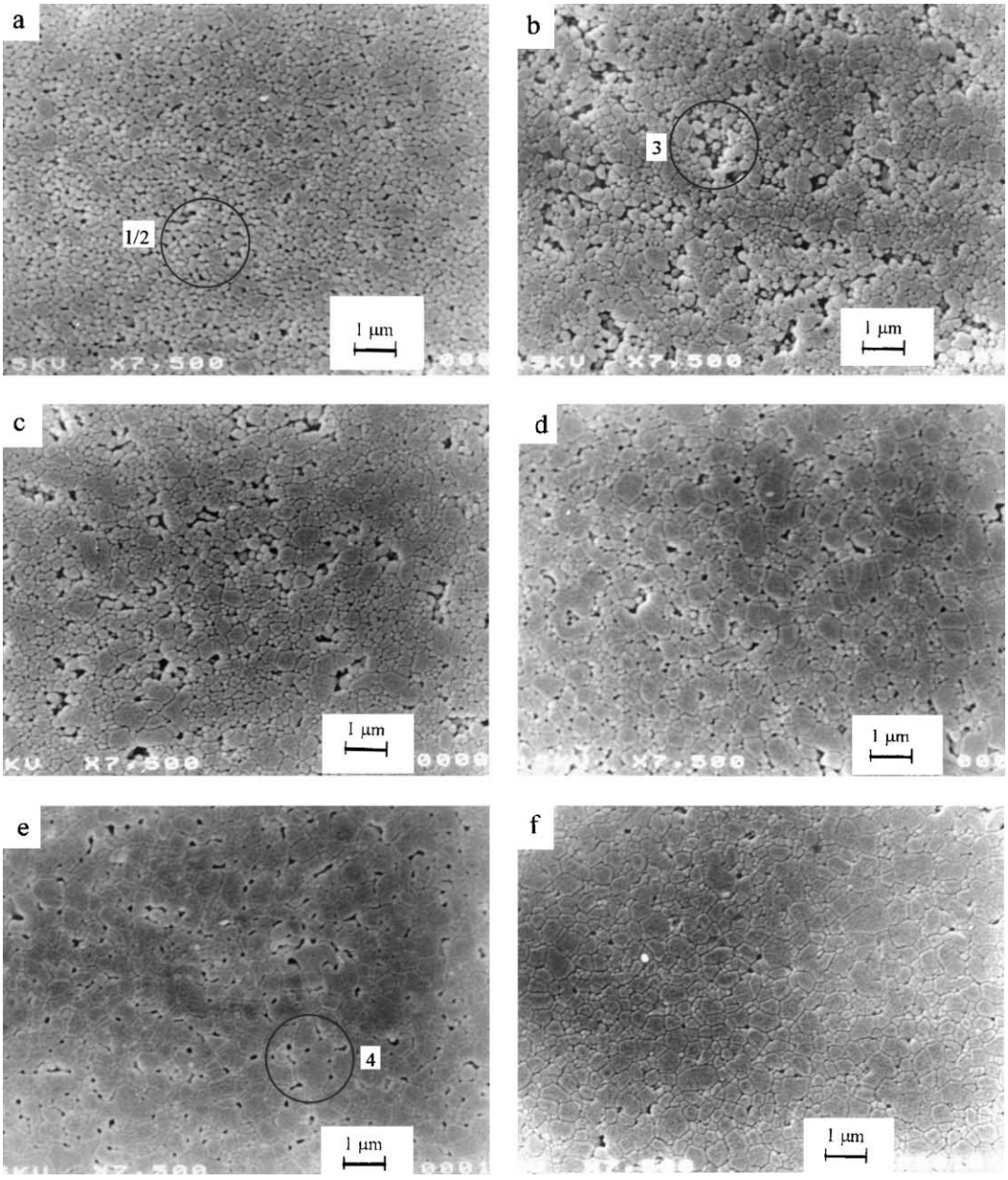

Fig. 7. Microstructure evolution of the compacts with GSD = 1.6 sintered at 1250 °C for different lengths of time: (a) 15 min (density = 74% th.); (b) 30 min (76% th.); (c) 60 min (80% th.); (d) 120 min (88% th.); (e) 150 min (90% th.), and (f) 240 min (92% th.). Examples of different types of pores are circled and marked accordingly.

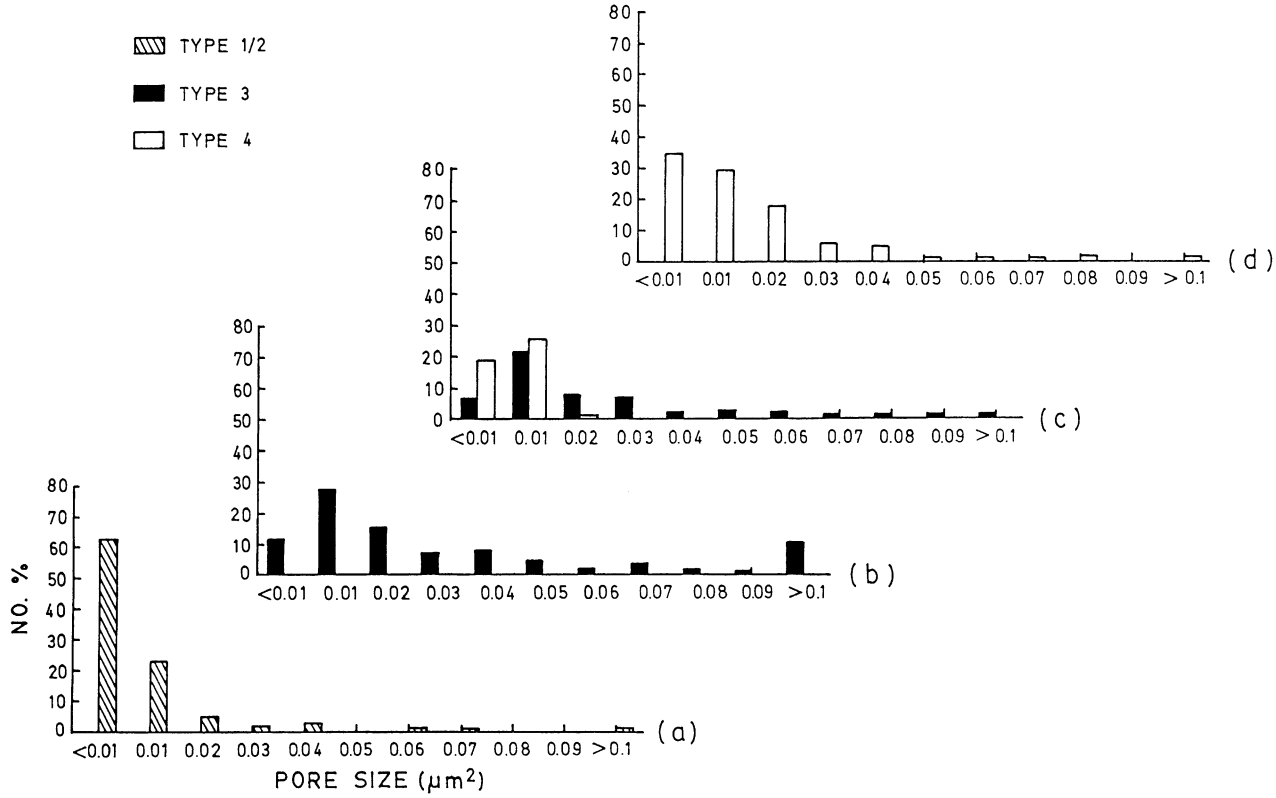

Fig. 8. Evolution of pore structures in the GSD = 1.2 compact sintered at 1250 °C: (a) 30 min (density = 70% th.); (b) 60 min (72% th.); (c) 120 min (78% th.) and (d) 240 min (80% th.).

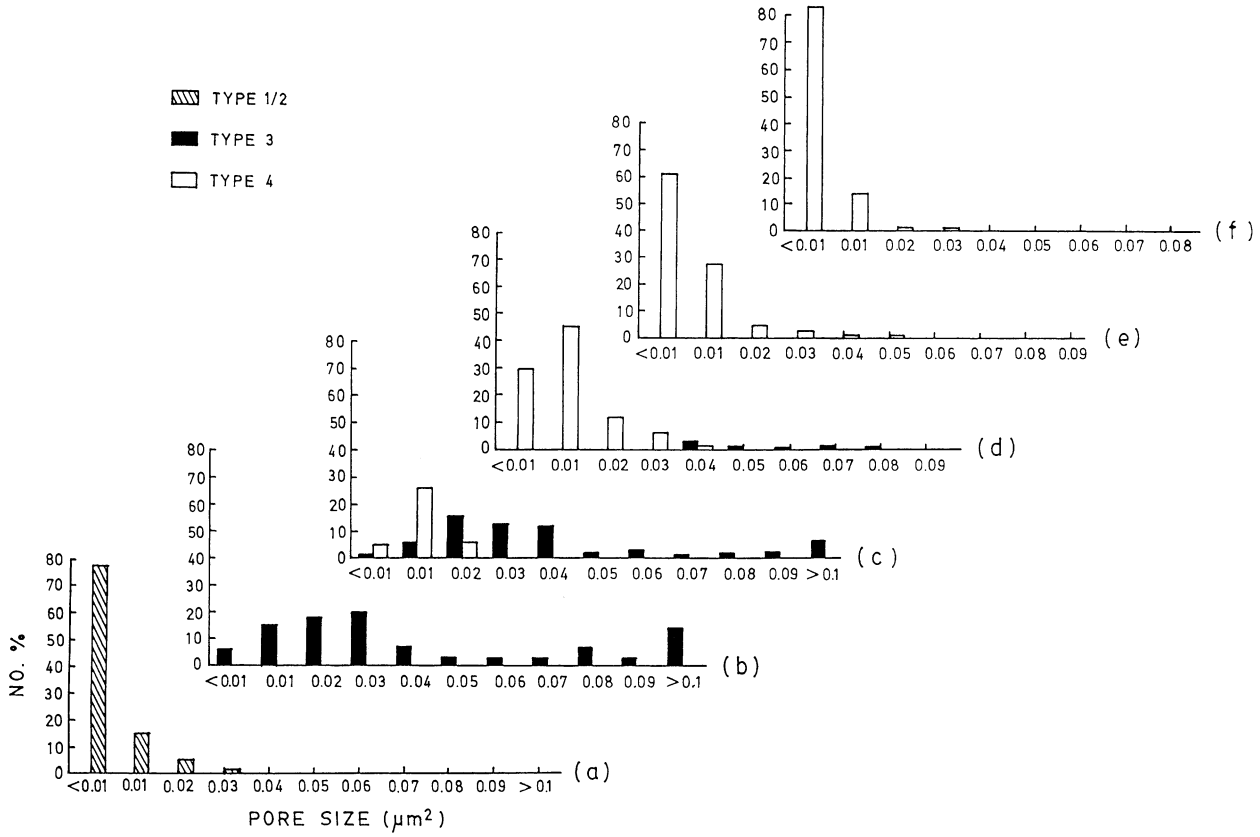

Fig. 9. Evolution of pore structures in the GSD = 1.6 compact sintered at 1250 °C: (a) 15 min (density = 74% th.) (b) 30 min (76% th.); (c) 60 min (80% th.); (d) 120 min (88% th.); (e) 150 min (90% th.), and (f) 240 min (92% th.).

4. Discussion

4.1. Beneficial effect of particle size distribution on sintering

The present work shows that when agglomerates are eliminated, the initial densification rate is enhanced appreciably with broader particle size distribution (Fig. 3). This can be attributed to the improved green density, hence a higher number of contact points among the particles, and the higher fractions of fine particles hence shorter diffusion paths, in the resultant compact. The broader size distribution powders also show enhanced grain growth during the intermediate stage of sintering (Fig. 5), which explains the faster drop in the densification rate observed in this stage of sintering.

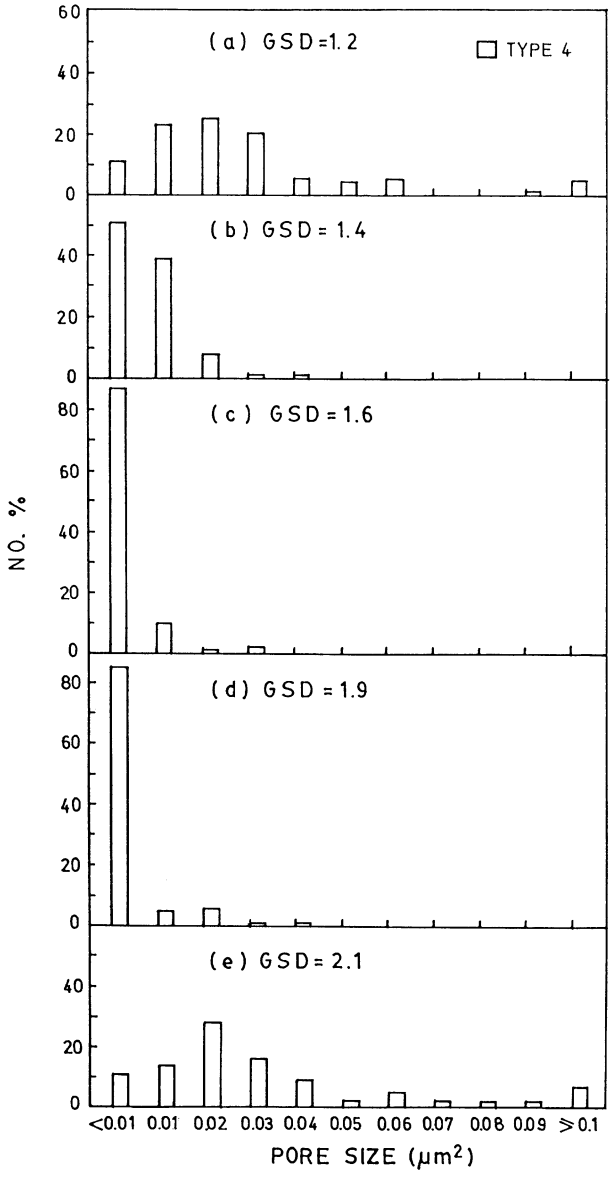

Fig. 10. Pore size distribution in various compacts at a density of 85% th.

This is because the densification rate of submicron alumina powder compacts is controlled by grain boundary diffusion,[22] which decreases with increasing average grain size of the compact.

As shown by Kingery and Francois,[23] Lange et al.[24] and Lim et al.,[22] grain growth is required for densification during the final stage of sintering when only isolated Type 4 pores are present. It is thus possible that the enhanced grain growth during the intermediate stage of sintering of the broader size distribution compacts could have modified the sintering characteristics of Type 4 pores and therefore the final-stage sintering behaviour of the compacts.

To check for the above, the densification and grain growth behaviours of the GSD = 1.2 and 1.6 compacts, sintered at a lower temperature of 1250 °C, were carefully studied. The results are shown in Fig. 11. Also shown in this figure are the types of pores formed at the various sintering stages. It can be noted that an appreciable amount of grain growth, promoted by the size distribution of the particles, had occurred in the compact with GSD = 1.6 during which Type 3 pores gradually developed into Type 4 pores (Fig. 11a). Therefore, the Type 4 pores formed in the GSD = 1.6 compact were embedded in a larger grained matrix, hence having

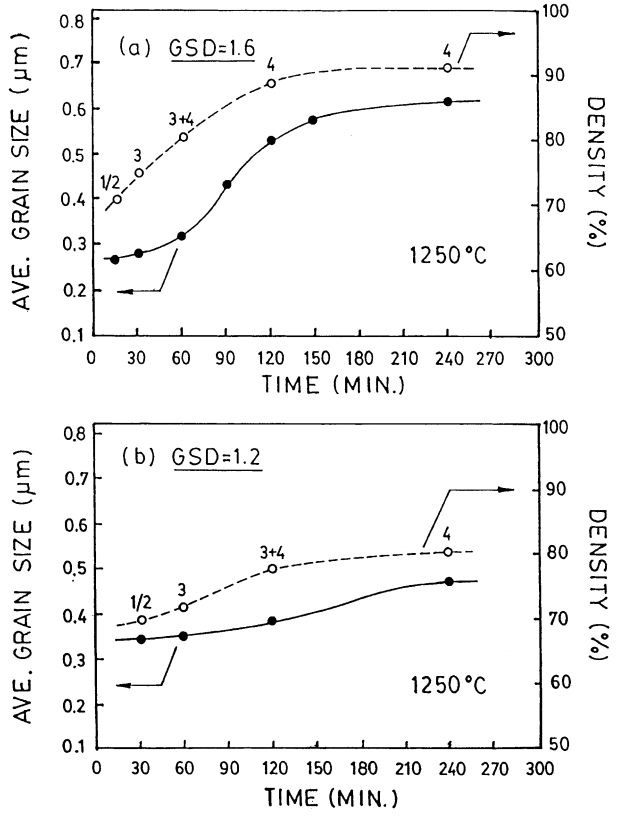

Fig. 11. Densification and grain growth curves at 1250 °C for compacts with (a) GSD = 1.6 and (b) GSD = 1.2. The figures within brackets indicate the dominant pore types at each density level.

smaller coordination numbers and higher sinterability. This is confirmed by the finer Type 4 pores detected in this compact (Fig. 10c). The high sinterability of Type 4 pores probably account for the relatively high densification rate in the final-stage sintering of this compact.

On the other hand, little grain growth was noted in the near-monosized (GSD = 1.2) compact at the intermediate stage of sintering (Fig. 11b). The Type 4 pores formed in this compact were thus embedded in a smaller grained matrix, and were not as highly sinterable due to their higher co-ordination numbers. This explains the distribution of Type 4 pores and the inferior sintering characteristics of the near-monosized compact (Fig. 10a).

The above finding is supported by the grain size-density trajectories shown in Fig. 6. It is evident from this figure that Type 4 pores in the GSD = 1.6 and 1.9 compacts are most sinterable in that a smaller amount of grain growth is required to bring about a given percentage change in density in these two compacts at the final stage of sintering (i.e. >90% relative density). On the other hand, Type 4 pores in the near-monosized (GSD = 1.2). compact are the least sinterable, while those in the GSD = 1.4 compact have intermediate sinterability. The reason for the decreased sinterability of the broadest size distribution powder compact will be discussed below.

Both densification and grain growth practically stopped after 2 h at 1250 °C. This is because upon the formation of Type 4 pores, concurrent grain growth is required for further sintering.[23,24] At this temperature, without the driving force provided by the particle size distribution, grain growth is sluggish and so is the densification rate in the final stage of sintering. This is consistent with the results obtained in our earlier work.[22]

4.2. Enhanced local differential densification

It is interesting to note from Fig. 4 that although the sintering characteristics of the compact with GSD = 2.1 remain superior to that of the near-monosized compact, it is significantly inferior to those of the compacts with GSD = 1.6 and 1.9. This holds despite the fact that the GSD = 2.1 compact registered the highest green density among all the compacts studied (Fig. 2) and that all these three compacts exhibited similar grain growth characteristics (Fig. 5). Examination of the microstructure of the compacts at different stages of sintering revealed that the GSD = 2.1 compacts had larger Type 4 pores compared with those of optimum size distributions (i.e. GSD = 1.6 and 1.9).

As the evolution of pores during sintering is intimately related to the green microstructure, one immediate question arises as if size segregation could have occurred during processing at sufficiently broad particle size distributions.

A check on the microstructure and experimental data revealed minimum possibility of macroscopic size segregation in the compact. Firstly, the supernatants after centrifugation were always clear. In fact, in one case the centrifugation was stopped before it reached the pre-set rotation speed. It was noted that the powder was already fully compacted with a clear supernatant. Secondly, scanning electron microscopy did not reveal noticeable evidence of size segregation across the thickness of the compacts. Thirdly, the green density of the GDS = 2.1 compact is the highest among all the size distributions studied. Should macroscopic size segregation be present, the green density of the compact would have been affected and will not continue to increase linearly with increasing width of particle size distribution. And, lastly, the pore structure of the GSD = 2.1 compact at 85% relative density is comparable to that of the near-monosized compact (Fig. 10). Minimum size segregation is to be expected in the latter compact due to the uniform size of starting particles used. Should size segregation be present, a noticeably coarser pore structure would have been formed in the GSD = 2.1 compact (as opposed to that of GSD = 1.2). This was not observed in the present work. Working with colloidally processed compacts made from similar alumina powders, Yeh and Sacks[21] also concluded from pore size measurements that no size segregation occurred in their compacts even for GSD = 2.4. In their work, the compacts were produced by slip casting from slurry of 50 vol.% solid loading.

Although macroscopic size segregation in the GSD = 2.1 compact can be ruled out, the larger Type 4 pores observed in this compact compared with those with optimum size distribution (i.e. GSD = 1.6 and 1.9), as evident in Fig. 10, strongly indicate that an increased degree of local differential sintering must have occurred in this compact. Such differential sintering effects have been known to be associated with variations in local particle packing, i.e. differences in coordination number of each particle and in the detailed arrangement of its neighbouring particles, in powder compacts.

In fact, variations in local particle packing also exist even in near-monosized powder compacts; and the ensuing differential densification has resulted in the agglomeration of particles during sintering of such compacts.[22] Therefore, despite the highest green density attained by the GSD = 2.1 compact, the different sizes of powder particles have given rise to an enhanced degree of variations in local particle packing in the compact. During subsequent sintering, the ensuing differential densification will lead to an enhanced degree of differential sintering via particle clustering and/or agglomeration. This, in turn, will lead to the formation of larger Type 3, hence Type 4, pores in the compact, as shown in Fig. 10. Similar observations were reported by earlier researchers.[17–19] It should, however, be noted that in these earlier works, the as-received broad size distribution powders, which were used as the reference

for comparison, also contained a small amount of agglomerates.

In other words, even in the absence of pre-existing agglomerates and macroscopic size segregation, two opposing events happen when the width of the particle size distribution of a powder compact is broadened. On one hand, enhanced densification occurs with increasing particle size distribution due to a higher green density and the formation of smaller Type 4 pores of higher sinterability, the latter being a result of enhanced grain growth during the intermediate stage. On the other hand, a higher degree of variations in local particle packing, hence extent of local differential densification, is also realised. With broader particle size distribution, the latter effect would become more and more pronounced, giving rise to a coarser pore structure in the sintering compact. This, in turn, would counter the beneficial effect of particle size distribution on sintering. Therefore, an optimum particle size distribution exists for best sinterability of powder compacts. For the agglomerate-free submicron alumina powders studied in the present work, the optimum particle size distributions were found to have a GSD value lying in between 1.6 to 1.9.

4.3. Comparison with predictions of Zhao and Harmer[39,41]

At this juncture, it should be mentioned that although most earlier models correctly predicted the enhanced densification rate during the initial stage of sintering[8,38,39] and the occurrence of early grain growth and its associated drop in sintering rate during the intermediate stage[8,27,39,40] with broader particle size distribution, they failed to address the phenomenon of enhanced local differential densification and the associated formation of larger second-generation (both Types 3 and 4) pores in the sintering compact. Most models also did not address how enhanced grain growth at intermediate stage brought about by the particle size distribution would affect the sinterability of pores at the final stage of sintering. In fact, most of the existing models predicted that the sinterablility of the compact decreases with broader particle size distribution,[8,39,40] which is at variance with the present observation.

One of the reported models which took into consideration the sinterability of pores at the final stage of sintering is that due to Zhao and Harmer.[41] They showed that when only highly-sinterable matrix pores are present, for a given compact density and pore number frequency, a fine pore structure having a narrow pore size distribution produces the most desirable grain size-density trajectory (see Fig. 12 of Ref. 41). This prediction is consistent with the present experimental observations, which show that compacts showing the highest sinterability and best grain size-density trajectories are those with a fine and narrow-size-distributed Type 4 pores (Fig. 10), which have a GSD value lying in between 1.6 and 1.9.

Despite the above agreement, it should be stressed that in the present work, the Type 4 pores are not the matrix pores as described in Zhao and Harmer's model. They are actually the remnants of second-generation pores formed as a result of sintering-induced agglomeration of particles in the initially agglomerate-free, homogeneous compact.

Zhao and Harmer[41] further reckoned that a fine and narrow-size distributed pore structure can be derived from powders with a narrow particle size distribution. This led them to conclude that near-monosized distribution powders are preferred for improved sinterability. As shown in the present work, in contrary to the their presumption, due to unavoidable sintering-induced agglomeration of particles, the resultant Type 4 pores are finer and of narrower size distribution in the compacts processed from powders of the optimum range of particle size distribution but not from near-monosized distribution powders (Fig. 10). In other words, highly sinterable compacts are obtained from powders of optimum size distribution but not from monosized powders, because nowadays it is not possible to arrange these particles free of defects. In case of an ideal packing, the sintering activity would be extremely homogeneous and no sintering-induced agglomerates or differential sintering would occur.

In a subsequent work, Zhao and Harmer[39] extended their model to study the microstructure development during sintering of compacts containing both first- and second-generation pores. In the said work, the second-generation pores were viewed as those produced by large, pre-existing agglomerates and it was shown that such pores cannot be removed easily even when grain growth is deliberately promoted in the compact, such as that brought about by a broad particle size distribution in the starting powder. This again led them to conclude that a near-monosized distribution of pores (or particles) is preferred for grain growth suppression and good sinterability of the resultant compact.

It should be mentioned that for initially agglomerate-free powder compacts, the size of the second-generation (Types 3 and 4) pores is determined by the degree of sintering-induced agglomeration in the compact, which in turn is controlled by the microstructural homogeneity in the green state. The latter is determined by the particle size and size distribution of the starting powder and the consolidation technique used. For compacts prepared colloidally from either monosized or narrow size distribution powders, the sintering-induced second-generation (Types 3 and 4) pores are much smaller in size with good sinterability, i.e. they can be sintered out at comparatively low temperatures.[22] The present work further showed that, in this case, the enhanced grain

growth at the intermediate stage of sintering brought about by broader particle size distribution does aid in the removal of such pores (Figs. 6 and 10), thus significantly improving the overall sinterability of the compact (Fig. 4). This is true provided that the increase in the degree of variations in local particle packing, hence sintering-induced agglomeration, brought about by the broader particle size distribution remains tolerable; such that the resultant second-generation (i.e. Type 3 and Type 4) pores are not too large and can be sintered out at relatively low temperatures with controlled grain growth. In other words, the model of Zhao and Harmer[39,41] can be used to describe the present result, on the condition that the second-generation pores are comparatively small and sinterable pores. In this context, one would expect that grain growth promoted by a broader particle size distribution would help in the removal of such pores, hence the sinterability of the compact, a conclusion which is different from that made in their original paper but verified by the present work.

The above suggests that the effect of particle size distribution on sintering depends, to a great extent, on the microstructural homogeneity of the green compact. For instance, as shown by Zhao and Harmer[39] and the present work, the conclusion regarding the effect of particle size distribution would be different when agglomerates are present in the starting compact. Similarly, any size segregation effect present in the compact may adversely negate the beneficial effects associated with a broader particle size distribution. Given the powder type, the uniformity in the green structure of a compact depends sensitively on the consolidation technique and conditions used. This means that the optimum particle size distribution for a given powder system would also vary depending on the consolidation technique and conditions used. In this regard, the authors are of the opinion that narrow size distribution powder is preferred to monosized or broad size distribution powders for controlling the sintering behaviour and resultant microstructure of powder compacts, provided that agglomerates in the starting powders are removed by appropriate means.

5. Conclusion

(a) Within the range of particle size distribution investigated (GSD = 1.2, 1.4, 1.6, 1.9 and 2.1), the green density of colloidally prepared fine-grained alumina powder compacts increases with particle size distribution. This leads to enhanced densification of the compacts at the initial stage of sintering.
(b) A broader particle size distribution also promotes grain growth during the intermediate stage of sintering, causing the densification rate at the intermediate stage to decrease more rapidly relative to that of near-monosized compacts.
(c) All powder compacts undergo similar microstructural changes during sintering, namely, local densification within clusters of particles leading to agglomeration and the formation of channel-like pores, their evolution into isolated pores, and the elimination of the latter on further sintering. A higher sintering temperature hastens the pace of microstructure evolution but not its stages of development.
(d) Due to enhanced grain growth at the intermediate stage, closed isolated (Type 4) pores in compacts processed from broader size distribution powders are embedded in a larger grained matrix, hence of better sinterability. This helps maintain a high sintering rate in the final stage and results in the superior sinterability of the broad size distribution compacts.
(e) A broader particle size distribution also results in an enhanced degree of variations in local particle packing, hence local differential densification, in the compact. Beyond a certain particle size distribution, this could result in a coarser pore structure in the sintering compact, which, in turn, would offset the beneficial effect on sintering brought about by particle size distribution.
(f) An optimum range of particle size distribution therefore exists for best sinterability for a given powder system. For the agglomerate-free, submicron alumina powder system studied, the optimum particle size distribution has a geometric standard deviation value lying in between 1.6 and 1.9.
(g) Within the range of particle size distribution investigated, the resultant grain size at the final stage of sintering is very much determined by the sintering condition used but not the particle size distribution of the starting powder.
(h) Even for a given powder system, the optimum particle size distribution may vary depending on the consolidation technique and conditions used. For practical purposes, narrow size distribution powder is thus preferred to monosized or broad size distribution powders for improved sinterability and high-reliability microstructure control of powder compacts, provided that agglomerates in the starting powders are removed by appropriate means.

Acknowledgements

The authors wish to acknowledge the financial support received from the European Communities, through

the Contract No. C11*-CT92–0047, and from the National University of Singapore for the provision of a research scholarship to J.M. They are also thankful to Sumitomo Chemicals Co., Japan, for the provision of the AKP powders used in the present work.

References

1. Yan, M. F., Microstructural control in the processing of electronic ceramics. *Mater. Sci. Eng*., 1981, **A48**, 53–72.
2. Barringer, E. A. and Bowen, H. K., Formation, packing and sintering of monodisperse TiO_2 powders. *J. Am. Ceram. Soc*., 1982, **65**, C199–C201.
3. Sacks, M. D. and Tseng, T. Y., Preparation of SiO_2 glass from model powder compacts: II, sintering. *J. Am. Ceram. Soc*., 1984, **67**, 532–537.
4. Sordelet, D. J. and Akinc, M., Sintering of monosized, spherical yttria powders. *J. Am. Ceram. Soc*., 1988, **71**, 1148–1153.
5. Patterson, B. R. and Benson, L. A., The effect of powder distribution on sintering. *Progress in Powder Metallurgy*, 1984, **39**, 215–230.
6. Patterson, B. R. and Griffin, J. A., Effect of particle size distribution on sintering of tungsten. *Mod. Des. Powd. Metall*., 1984, **15**, 279–288.
7. Ting, J. M. and Lin, R. Y., Effect of particle-size distribution on sintering. Part II. Sintering of alumina. *J. Mater. Sci*., 1995, **30**, 2382–2389.
8. Ting, J. M. and Lin, R. Y., Effect of particle-size distribution on sintering. Part I Modelling. *J. Mater. Sci*., 1994, **29**, 1867–1872.
9. Rhodes, W. H., Agglomerate and particle size effects on sintering yttria-stablised zirconia. *J. Am. Ceram. Soc*., 1981, **64**, 19–22.
10. Lange, F. F., Sinterability of agglomerated powders. *J. Am. Ceram. Soc*., 1984, **67**, 83–89.
11. Hsueh, C. H., Evans, A. G., Cannon, R. M. and Brook, R. J., Viscoelastic stresses and sintering damage in heterogeneous powder compacts. *Acta Metall*., 1986, **34**, 927–936.
12. Kimura, T., Matsuda, Y., Oda, M. and Yamaguchi, T., Effect of agglomerates on the sintering of alpha-Al_2O_3. *Ceram. Int*., 1987, **13**, 27–34.
13. Carter, W. C. and Cannon, R. M., Sintering microstructures: instabilities and the interdependence of mass transport mechanisms. In *Ceramic Transaction,* Vol. 7*, Sintering of Advanced Ceramics*, ed. C. A. Handwerker, J. Blendell and W. Kayser. American Ceramic Society, Westerville, OH, 1989, pp. 137.
14. Aksay, I. A., Microstructure control through colloidal consolidation. In *Advances in Ceramics,* Vol. 19, ed. J. A. Mangels and G. L. Messing. American Ceramic Society, Columbus, OH, 1984, pp. 94–104.
15. Yeh, T. S. and Sacks, M. D., Low temperature sintering of aluminum oxide. *J. Am. Ceram. Soc*., 1988, **71**, 841–844.
16. Cameron, C. P. and Raj, R., Grain growth transition during sintering of colloidally prepared alumina powder compacts. *J. Am. Ceram. Soc*., 1988, **71**, 1031–1035.
17. Roosen, A. and Bowen, H. K., Influence of various consolidation techniques on the green microstructure and sintering behavior of alumina powder. *J. Am. Ceram. Soc*., 1988, **71**, 970–977.
18. Hay, R. H., Moffatt, W. C. and Bowen, H. K., Sintering behaviour of uniform-sized α-Al_2O_3. *Mater. Sci. Eng*., 1989, **A108**, 213–219.
19. Shiau, F. S., Fang, T. T. and Leu, T. S., Effect of particle size distribution on the microstructural evolution in the intermediate stage of sintering. *J. Am. Ceram. Soc*., 1997, **80**, 286–290.
20. Lim, L. C., Wong, P. M. and Ma, J., Colloidal processing of submicron alumina powder compacts. *J. Mater. Proc. Technol*., 1997, **67**, 137–142.
21. Yeh, T. S. and Sacks, M. D., Effect of particle size distribution on the sintering of alumina. *J. Am. Ceram. Soc*., 1988, **71**, C484–C487.
22. Lim, L. C., Ma, J. and Wong, P. M., Microstructural evolution during sintering of near-monosized agglomerate-free submicron alumina powder compacts. *Acta Mater*., 2000, **48**, 2263–2275.
23. Kingery, W. D. and Francois, B., The sintering of crystalline oxides I: interaction between grain boundaries and pores. In *Sintering and Related Phenomena*, ed. G. C. Kuczynske, N. A. Hooton and G. F. Gibbon. Gordon and Breach, New York, 1967, pp. 471–498.
24. Kellet, B. J. and Lange, F. F., Thermodynamics of densification: I, sintering of simple arrays, equilibrium configurations, pore stability, and shrinkage. *J. Am. Ceram. Soc*., 1989, **72**, 725–734 and 735–741.
25. Hillert, M., On the theory of normal and abnormal grain growth. *Acta Metall*., 1965, **13**, 227–238.
26. Brook, R. J., Controlled grain growth in ceramic systems. In *Treatise on Materials Science and Technology,* Vol. 9, ed. F. F. Y. Wand. Academic Press, New York, 1976, pp. 331–364.
27. Yan, M. F., Cannon, R. M., Bowen, H. K. and Chowdry, U., Effect of grain size distribution on sintering density. *Mater. Sci. Eng*., 1983, **A60**, 275–281.
28. Onada, G. Y. Jr., Green body characteristics and their relationship to finished microstructures. In *Ceramic Microstructures '76*, ed. R. M. Fulrath and J. A. Pask. Westview Press, Boulder, CO, 1977, pp. 183–183.
29. Messing, G. L. and Onoda, G. Y. Jr., Inhomogeneity-packing density relations in binary powders. *J. Am. Ceram. Soc*., 1978, **61**, 1–5.
30. Smith, J. P. and Messing, G. L., Sintering of bimodally distributed alumina powders. *J. Am. Ceram. Soc*., 1984, **67**, 238–242.
31. Liniger, E. and Raj, R., Packing and sintering of two dimensional structures made from bimodal particle size distributions. *J. Am. Ceram. Soc*., 1987, **70**, 843–849.
32. Lange, F. F., Powder processing science and technology for increased reliability. *J. Am. Ceram. Soc*., 1989, **72**, 3–15.
33. Chang, J. C., Velamakanni, B. W., Lange, F. F. and Pearson, D. S., Centrifugal consolidation of Al_2O_3/ZrO_2 composite slurries vs interparticle potentials: particle packing and mass segregation. *J. Am. Ceram. Soc*., 1991, **74**, 2201–2204.
34. Bordia, R. K. and Scherer, G. N., On constrained sintering. I. Constitutive model for a sintering body. *Acta Metall. Mater*., 1988, **36**, 2393–2397.
35. Du, Z. Z. and Cocks, A. C. F., Constitutive models for the sintering of ceramic components—I. Material Models. *Acta Metall. Mater*., 1992, **40**, 1969–1979.
36. Du, Z. Z. and Cocks, A. C. F., Constitutive models for the sintering of ceramic components—II. Sintering of inhomogeneous bodies. *Acta Metall. Mater*., 1992, **40**, 1969–1979.
37. Cocks, A. C. F., Overview No. 117: The structure of constitutive laws for the sintering of fine grained materials. *Acta Metall. Mater*., 1994, **42**, 2191–2210.
38. Coble, R. L., *J. Am. Ceram. Soc*., 1973, **56**, 461.
39. Zhao, J. and Harmer, M. P., Effect of pore distribution on microstructure development: II, first- and second-generation pores. *J. Am. Ceram. Soc*., 1988, **71**, 530–539.
40. Chappell, J. S., Ring, T. A. and Birchall, J. D., Particle size distribution effects on sintering rates. *J. Appl. Phys*., 1986, **60**, 383–391.
41. Zhao, J. and Harmer, M. P., Effect of pore distribution on microstructure development: I, matrix pores. *J. Am. Ceram. Soc*., 1988, **71**, 113–120.